Rev. Adv. Mater. Sci. 38 (2014) 17-28

GRAIN BOUNDARY PHENOMENA IN NdFeB-BASED HARD MAGNETIC ALLOYS

B.B. Straumal[1,2], A.A. Mazilkin[1], S.G. Protasova[1], A.M. Gusak[3], M.F. Bulatov[4], A.B. Straumal[1,5] and B. Baretzky[2]

[1]Institute of Solid State Physics, Russian Academy of Sciences, 142432 Chernogolovka, Russia
[2]Karlsruhe Institute for Technology (KIT), Institute for Nanotechnology, Hermann-von-Helmholtz-Platz 1, 76344 Eggenstein-Leopoldshafen, Germany
[3]Department of Theoretical Physics, Cherkasy National University, Shevchenko blvd. 81, 18027 Cherkasy, Ukraine
[4]Federal State Research and Design Institute of Rare Metal Industry ("Giredmet"), B. Tolmachevsky lane 5-1, 119017 Moscow, Russia
[5]National Research University of Technology "MISiS", Leninskiy prosp. 4, 119049 Moscow, Russia

Received: January 24, 2014

Abstract. The NdFeB-based alloys were invented in 1980-ies and remain the best known hard magnetic alloys with highest magnetic energy product. The unique properties of NdFeB-based alloys are due to the thin layers of a magnetically isolating Nd-rich phase in grain boundaries (GB) and triple junctions (TJs). The prewetting (or premelting) phase transitions were the first reasons permitted to explain their existence. The deficit of the wetting phase in case of complete wetting can also lead to the formation of thin GB and TJ phases. However, only the phenomenon of pseudopartial (or pseudoincomplete, or constrained complete) wetting permitted to explain, how the thin GB film can exist in the equilibrium with GB lenses of a second phase with non-zero contact angle. The focused usage of such thin magnetically isolating GB layers can further improve the properties of NdFeB-based hard magnetic alloys.

1. INTRODUCTION

The NdFeB-based alloys were invented in 1980-ies. They remain the best known hard magnetic alloys with highest magnetic energy product *HB* (*B* being the flux density and *H* being the field strength). In order to reach the optimum magnetic properties the $Nd_2Fe_{14}B$ grains has to be isolated one from another by the layers of a non-ferromagnetic phase. In most cases it is the Nd-rich phase. It forms during the liquid-phase sintering as liquid layer between $Nd_2Fe_{14}B$ grains formed. It has been demonstrated rather early [1] that the thickness of these layers needed for effective magnetic isolation between $Nd_2Fe_{14}B$ grains is only few nanometers [2]. If the total amount of the Nd-rich phase is too high, it decreases the saturation magnetization of an alloy as a whole. Therefore, the amount of the Nd-rich phase has to be kept as low as possible, namely at the level which is minimally needed for the effective magnetic isolation between grains of the hard magnetic $Nd_2Fe_{14}B$ phase. It is the big challenge for the materials science. This goal can be reached by the smart tailoring of grain boundary (GB) wetting. It can be made using the knowledge of the GB and

Corresponding author: B.B. Straumal, e-mail: straumal@issp.ac.ru

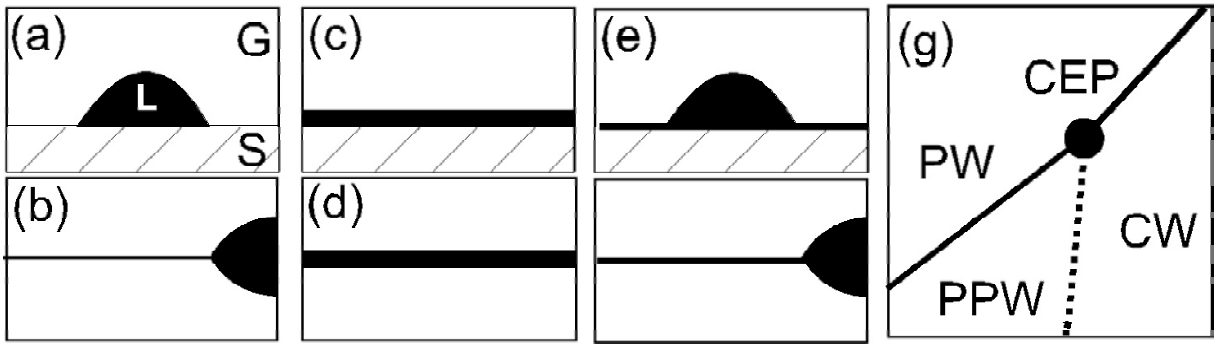

Fig. 1. The schemes for the wetting of free surfaces and GBs. (a) partial surface wetting, L – liquid phase, S – solid phase, G – gas phase; (b) partial GB wetting; (c) complete surface wetting; (d) complete GB wetting; (e) pseudopartial surface wetting; (f) pseudopartial GB wetting; (g) generic wetting phase diagram proposed in [25], PW – partial wetting, CW – complete wetting, PPW – pseudopartial wetting, CEP – critical end point, thick lines mark the discontinuous (first order) wetting transition, thin line mark the continuous (second order) wetting transition.

triple junctions (TJs) wetting phenomena like complete, partial, pseudopartial wetting, prewetting, premelting, etc. The most advanced experimental methods like high-resolution electron microscopy (HREM) and atom probe microscopy allowed observing that GBs and TJs are frequently not atomically thin and smooth but contain the few nm thick layers or so-called complexions [3–13]. These layers can appear in equilibrium, non-equilibrium (transient) or steady-state structures [4–22]. The goal of this paper is to review the main classes of these GB and TJ phenomena and their possible applications for further development of NdFeB-based alloys.

2. THERMODYNAMIC REASONS FOR THE EXISTENCE OF GB AND TJ THIN LAYERS

Let us consider a partially melted two- or multicomponent polycrystal. In this case its temperature is between the solidus temperature T_S and the liquidus temperature T_L, in the equilibrium phase diagram. Consider the droplet of a liquid phase on the surface of a solid phase or between two solid grains. Usually one distinguishes partial and complete wetting of surfaces or interfaces. If a liquid droplet partially wets a solid surface (Fig. 1a) then $\sigma_{sg} - \sigma_{sl} = \sigma_{lg} \cos\theta$, where σ_{sg} is the free energy of solid/gas interface, σ_{sl} is the free energy of solid/liquid interface, σ_{lg} is that of liquid/gas interface and θ is the contact angle. If a liquid droplet partially wets the boundary between two solid grains (Fig. 1b), then $\sigma_{gb} = 2\,\sigma_{sl} \cos\theta$, where σ_{gb} is the free energy of a grain boundary (GB). The free surface or GB which is not covered by the liquid droplets remains dry and contains only the adsorbed atoms with coverage below one monolayer. In this case the GB can exist in the equilibrium contact with the liquid phase (GBs marked with a letter A in Fig. 2). In the case of complete wetting (Figs. 1c and 1d) $\sigma_{sg} > \sigma_{lg} + \sigma_{sl}$ or $\sigma_{gb} > 2\sigma_{sl}$, the contact angle is zero, and liquid spreads over the free surface or between grains. In this case the GB separating the grains is completely substituted by the liquid phase (GBs marked with a letter B in Fig. 2). The GB wetting phenomena are

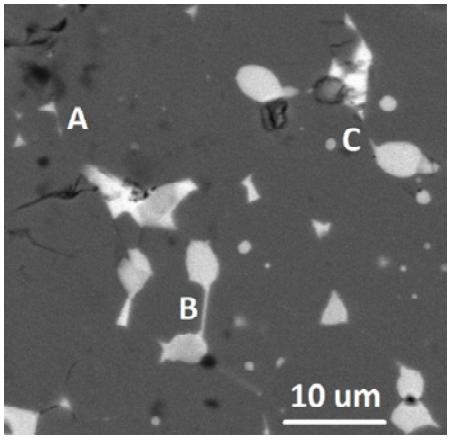

Fig. 2. The microstructure (SEM) of the liquid phase sintered Nd-Fe-B-Co-Cu commercial alloy after additional annealing at 700 °C, 2 h. The $Nd_2Fe_{14}B$ solid grains appear dark. The (solidified after quenching) Nd-rich liquid phase appears light. **A:** $Nd_2Fe_{14}B$/$Nd_2Fe_{14}B$ GB incompletely wetted by the melt. **B:** $Nd_2Fe_{14}B$/$Nd_2Fe_{14}B$ GB completely wetted by the melt. **C:** $Nd_2Fe_{14}B$/$Nd_2Fe_{14}B$ GB incompletely wetted by the melt, non-zero contact angle. However, the liquid layers from TJs almost meet in the middle of the Cu/Cu GB.

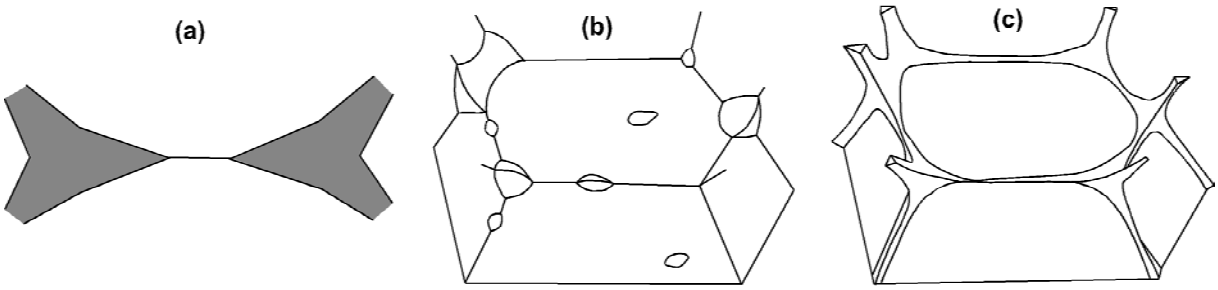

Fig. 3. (a) Scheme of the apparently complete GB wetting. The liquid layers "meet each other" in a GB between TJs even by $\theta > 0°$. (b) Liquid droplets in GBs and TJs. (c) Liquid phase in GB triple junctions forms a continuous network of liquid channels, [35]. Reprinted with permission from Elsevier Ltd., © 1975 Pergamon Press Ltd.

particularly important for the liquid phase sintering [23,24].

The correct experimental measurement of the contact angle θ is not an easy task. The most accurate measurement of a dihedral contact angle θ is possible in the experiments with bicrystals [26,27]. In this case θ is measured in the section perpendicular to the flat individual GB and to the straight contact line between the GB and the liquid phase. In polycrystals the correct measurement of θ is much more complicated. If a GB contains lenticular liquid droplets, they are formed by two spherical solid/liquid interfaces. The correct θ value appears only in the section containing the common axis of both spherical solid/liquid interfaces. It can be measured either using transmission electron microscopy (TEM) [28] or by careful three-dimensional analysis of the droplet shape [29,30]. Moreover, the energy of GBs and interphase boundaries strongly depend on their misorientation and inclination parameters [31–33]. Therefore, also the θ values are different for different GBs in polycrystals. Even if all GBs would have the same energy and the same dihedral angle with the liquid phase, the conventional metallographic (or ceramographic, or petrographic) section would cross the lenticular particles in a random way. This would result in a certain scatter of measured θ values around the true values of the dihedral contact angle. If the amount of the liquid phase is large, melted layers would separate the solid grains even if the contact angle $\theta > 0°$. This phenomenon is called *apparently complete GB wetting* [34]. In the case of apparently complete GB wetting the liquid layers "meet each other" in a GB between TJs even by $\theta > 0°$ (see GB marked by the letter C in Fig. 2 and scheme in Fig. 3a). The apparently complete GB wetting phenomenon increases the percentage P_{app} of completely wetted GBs over and above the equilibrium value P_{equ}.

Similar phenomenon is responsible for the formation of liquid channels along TJs. The dependence of microstructure of semi-solid polycrystals on the amount of liquid phase has been discussed for many years. Beere demonstrated that the gaseous or liquid phase in GB triple junctions forms a continuous network if its volume fraction is above a certain threshold value (see scheme in Fig. 3c) [35]. The threshold volume fraction varies with dihedral angle and increases with increasing θ [35,36]. For example, for a dihedral angle of 15° already 2% of liquid phase is enough to connect all quadruple points by liquid channels (In a quadruple point four grains contact each other and three triple junctions cross). For the microstructure of liquid-phase sintered materials, a quantity known as the contiguity parameter has been defined [37,38]. This is a quantitative measure of interphase contact, and is defined as the fraction of internal surface area of a phase shared with grains of the same phase in a two-phase microstructure. In liquid-phase sintering, these contacts serve a useful role in providing rigidity to a sintered compact, thereby controlling shape distortion. The contiguity depends strongly on the volume fraction of the solid phase and the dihedral angle; it increases with both parameters. At low dihedral angles, the contiguity increases rapidly as the volume fraction of the solid phase approaches unity [37]. Jurewicz and Watson defined the so-called equilibrium melt fraction which represents a minimum interfacial energy state when the melt is distributed uniformly along triple junctions in a partly-melted polycrystal [39]. The equilibrium melt fraction decreases with increasing θ. For example, it is only 2% for $\theta = 40°$ [39]. The θ value also influences the early stages of liquid-phase sintering when individual grains "swim" in a melt and form the first contact necks [40]. Similar observation were made also by investigations of ice melting and sintering of $ZnO–Bi_2O_3$ powders [3,15,41–43].

The transition from incomplete to complete GB wetting proceeds at a certain T_w if the energy of two solid-liquid interfaces $2\sigma_{SL}$ becomes lower than the

GB energy $\sigma_{GB} > 2\ \sigma_{SL}$. Cahn [44] and Ebner and Saam [45] first showed that the (reversible) transition from incomplete to complete wetting can proceed with increasing temperature, and that it is a true surface phase transformation. The GB wetting temperatures T_w, depend both on GB energy and solid-liquid interfacial energy which, in turn, depend on the crystallography of these interfaces [31,46–48]. The transition from incomplete to complete GB wetting starts at a certain minimum temperature T_{wmin} which corresponds to the combination of maximum σ_{GB} and minimum σ_{SL}. The transition from incomplete to complete GB wetting finishes at a maximum temperature T_{wmax} which corresponds to the combination of minimum σ_{GB} and maximum σ_{SL}. The fraction of completely wetted GBs increases from 0 to 100% as the temperature increases from T_{wmin} to T_{wmax} [49–55]. As a result, the new tie-lines appear in the S+L area of a phase diagram at T_{wmin} and T_{wmax} [49–55]. Due to the simple geometric reasons, the wetting transition in TJs proceeds at T_{wTJ} which is below the T_{wmin} for GBs [56]. The wetting transition for the low-angle GBs proceeds at T_{wLA} which is above the T_{wmax} for high-angle GBs [33]. GBs can also be "wetted" by a second solid phase [57–63].

If the alloys are *slightly below the solidus line*, i.e. in the solid-solution area of the bulk phase diagram (marked as *3* in Fig. 4), a thin layer of the liquid-like phase can be formed in GBs. In this area the liquid phase can appear in the GBs even though it is metastable in the bulk [16–18, 64]. This is because the system needs the additional energy ΔG for the formation of a metastable liquid phase. This energy can be compensated if the condition of full wetting, $\sigma_{GB} > 2\sigma_{SL}$, is fulfilled and the energy gain $\sigma_{GB} - 2\sigma_{SL}$ is higher than the energy loss ΔG. In this case a thin layer of a liquid-like phase may appear in the GB. The concentration of the second component in the liquid-like phase is also given by the liquidus line at the respective annealing temperature.

If the alloys are *deeply below the solidus line* in the solid-solution area of the bulk phase diagram (area *4* in Fig. 4), ΔG further increases and $\sigma_{GB} - 2\sigma_{SL}$ cannot compensate ΔG any more. The liquid-like GB layer disappears below GB solidus line (thin line in Fig. 4). GB solidus begins at the melting point T_m of the pure component. GB solidus finishes at the intersection between GB wetting tie-line and bulk solidus. Each GB with its σ_{GB} has its own wetting tie-line and respective GB solidus. Only one (hypothetic) GB solidus line corresponding to maximal GB energy σ_{GBmax} and minimal $T_{w0\%}$ is drawn in Fig. 4.

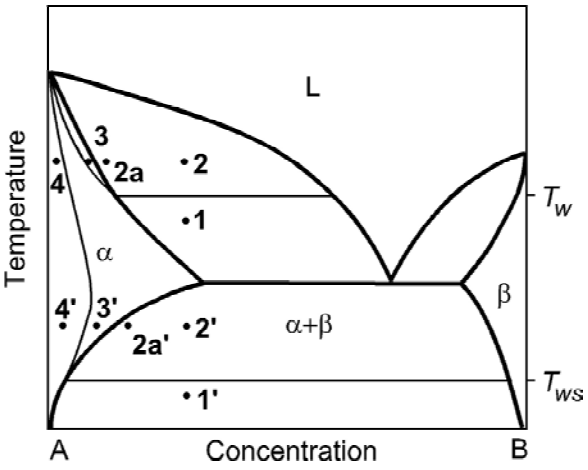

Fig. 4. Schematic phase diagram with lines of GB phase transitions. T_w – temperature of the GB wetting phase transition (proceeds between points 1 and 2). T_{ws} – temperature of the GB solid phase wetting transition (proceeds between points 1' and 2'). Between points 3 and 4 the GB premelting phase transition occurs. Between points 3' and 4' the GB prewetting phase transition occurs. In points 3 and 3' GB is covered by the equilibrium layer of a liquid-like or β-like phase which is unstable in the bulk. In points 2a and 2a' the wetting phase is in a deficit and cannot cover the GB with a thick layer. As a result GB is covered by the thin layer of a phase similar to that in points 3 and 3'.

Such phenomenon is called prewetting or premelting. It has been first predicted by Cahn [44]. It can exist also if the second phase is solid. In the point *2'* (Fig. 4) GB in the α-phase has to be substituted by the layer of β-phase and two α/β interphase boundaries (IBs). In the point *3'* GB is covered by the equilibrium layer of a β-like phase which is unstable in the bulk. In the points *4* and *4'* (Fig. 4) GB is "pure" and contains only the usual segregation layer of component B.

The GB premelting/prewetting phenomenon was observed for the first time by the investigations of zinc diffusion along the individual GBs in Fe–Si bicristals [26, 65–70]. Zn-based melt wets the GBs in all studied Fe-based alloys with 5, 10, 12.5, and 14 wt.% Zn. In the experiments the amount of liquid phase was chosen in such a way that it penetrated only to a certain depth. Below this depth the sample contained only one phase, namely the bcc-Fe with solved Zn. Close to the solubility limit (solvus) c_s of Zn in bcc-Fe the diffusivity of Zn atoms in GB was very high. The GB Zn diffusivity suddenly dropped to the conventional values at a certain concentration c_{bt}. The accelerated Zn GB diffusion has been

explained by the formation of GB premelting/prewetting layer between c_s and c_{bt} [26, 65–70]. By increasing pressure the GB wetting disappears, the accelerated GB diffusion along the premelting/prewetting GB layer disappears as well [26,69]. The $c_{bt}(T)$ premelting/prewetting lines have been constructed for the Fe-based alloys with 5, 10, 12.5, and 14 wt.% Zn [70]. The magnetic and/or chemical ordering in these alloys induces the additional attractive force between both grains, it leads to the disappearance of the GB premelting/prewetting together with accelerated GB zinc diffusion.

In the case of complete wetting (Figs. 1c and 1d) $\sigma_{sg} > \sigma_{lg} + \sigma_{sl}$ or $\sigma_{gb} > 2\,\sigma_{sl}$, the contact angle is zero, and liquid spreads over the free surface or between grains. What happens, if the amount of liquid is small and surface (or GB) area is large? In this case the liquid spreads until both solid grains or solid and gas begin to interact with each other through the liquid layer. The liquid forms a "pancake" with a thickness e_s of about 2-5 nm [8,71]:

$$e_s = \left(A / 4\pi S\right)^{1/2}, \qquad (1)$$

where $S = \sigma_{sg} - \sigma_{sl} - \sigma_{lg}$ is the spreading coefficient on a strictly "dry" solid and A is the Hamaker constant [72]. In case of complete wetting $A > 0$ and $S > 0$ [71]. Such "pancake" on the free surface or between the grains is formed by the deficit of a wetting phase, i.e. in the $\alpha + L$ or $\alpha + \beta$ two-phase area of a phase diagram, but very close to the solidus or solvus line. This "pancake" is very similar to the prewetting or premelting thin films which form also very close to the solidus or solvus line, but on the other side of it, namely in the one-phase area α (points *2a* and *2a'*).

It has been shown that the transition from partial to complete wetting is the surface phase transformation [44,45]. In the majority of cases the direct transition occurs from partial wetting (PW in the generic phase diagram Fig. 1g, proposed in Ref. 25) into complete wetting (CW), for example by increasing temperature [48,52,73] or decreasing pressure [74]. However, in some cases the state of pseudopartial (or pseudoincomplete, or constrained complete) wetting occurs (PPW in Fig. 1g) between partial and complete wetting. In this case the contact angle $\theta > 0$, the liquid droplet does not spread over the substrate, but the thin (few nm) precursor film exists around the droplet and separates substrate and gas (Fig. 1e). Such precursor film is very similar for the liquid "pancake" in case of complete wetting and deficit of the liquid phase (see above). This case is called pseudopartial wetting, it is possible when $A < 0$ and $S > 0$ [71]. In case of pseudopartial wetting the precursor exists together with liquid droplets, and in case of complete wetting the droplets disappear forming the "pancake".

The sequence of discontinous PW↔PPW and continuous PPW↔CW has been observed for the first time in the alcanes/water mixture [25]. The critical end point (CEP) was observed in a mixture of pentane and hexane which was deposited on an aqueous solution of glucose [25]. The first direct measurement of the contact angle in the intermediate wetting state (pseudo-partial wetting) was performed in the sequential-wetting scenario of hexane on salt brine [25]. Later the formation of Pb, Bi and binary Pb–Bi precursors surrounding liquid or solidified droplets has been observed on the surface of solid copper [75]. The pseudopartial wetting should in principle exist also for GBs (Fig. 1f). It has been observed for example in Al–Zn alloys after severe plastic deformation [76]. The contact angle between Zn particles and Al/Al GBs is above 60°. However, about one third of Al/Al GBs in the polycrystal contains the 2-3 nm thick Zn-enriched layers.

However, if one observes the thin GB layers of a constant thickness (also called complexions), it is not easy to distinguish, whether one has the case of (1) prewetting/prewetting in the one-phase area of a bulk phase diagram; (2) thin GB "pancake" due to the deficit of wetting phase or (3) pseudopartial wetting by a liquid or solid phase. The big problem is that most frequently the bulk liquid or solid phase can be found only in the TJ "pockets". The pseudopartial wetting can be clearly identified only if the contact angle $\theta \geq 60°$ and the solid/liquid interface is convex (Figs. 5a and 5b) . If the contact angle $\theta < 60°$ and the solid/liquid interface is concave (Figs. 5c and 5d), the difference becomes very fine. If the solid/liquid interface has a discontinuity (two tangentials) between TJ pocket and GB layer (Figs. 5c), the pseudopartial wetting takes place. If the solid/liquid interface is continuous (one tangential) between TJ pocket and GB layer (Figs. 5d), the complete wetting with the deficit of wetting phase takes place. In the next sections we will discuss these possibilities for various systems.

3. BEHAVIOR OF GB LAYERS AND TJ CHANNELS IN NdFeB-BASED ALLOYS

The most broadly used technology for the production of NdFeB-base hard magnetic alloys is the liquid phase sintering of a rather coarse-grained

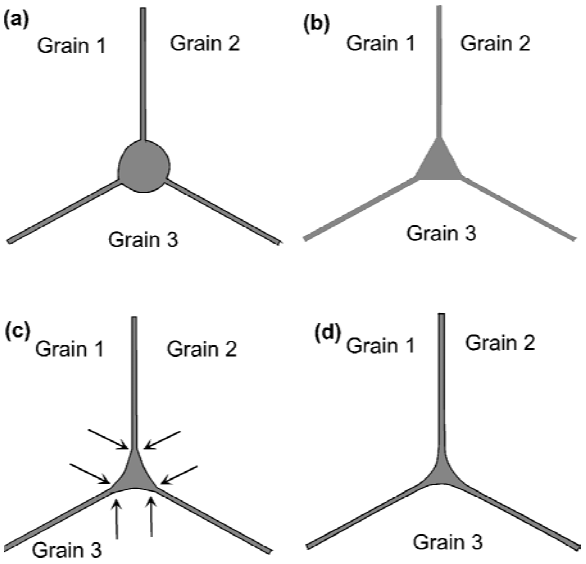

Fig. 5. Different configurations of liquid phase in the GB triple junction and thin quasi-liquid thin layers in the GB. (a) Pseudopartial GB wetting, $\theta > 60°$. (b) Pseudopartial GB wetting, $\theta = 60°$. (c) Pseudopartial GB wetting, $\theta < 60°$. The contact points between liquid phase in TJ and quasi-liquid layers in the GB are shown by arrows. (d) Complete GB wetting, $\theta = 0°$.

(10-20 μm) $Nd_2Fe_{14}B$ powders. The liquid phase sintering usually proceeds close to 1100 °C [23,24]. It would be logically to suppose that at this high temperature the liquid phase completely wets the boundaries between $Nd_2Fe_{14}B$ grains and prevents them to agglomerate with each other and to form the $Nd_2Fe_{14}B$/ $Nd_2Fe_{14}B$ GBs. In order to check this apparently obvious fact, the contact angles between melt and the $Nd_2Fe_{14}B$/$Nd_2Fe_{14}B$ GBs were experimentally measured in the temperature interval between 700 and 1100 °C [77]. However, even at highest studied temperature of 1100 °C the portion of completely wetted $Nd_2Fe_{14}B$/$Nd_2Fe_{14}B$ GBs was slightly above 80%. It quickly decreased with decreasing temperature, and at 700 °C GBs it was only around 10%. These results concern the „pure" three-component Nd–Fe–B alloys. The micrographs published in the literature permitted us to estimate the amount of completely wetted $Nd_2Fe_{14}B$/$Nd_2Fe_{14}B$ GBs in the alloys containing various alloying elements (like Dy, Pr, Al, Cu, Co etc.) in addition to Nd, Fe, and B. The amount of completely wetted GBs was astonishingly low in these cases. Very seldom the data points were above the line for three-component Nd–Fe–B alloys. In some cases the portion of completely wetted GB was around 20% even at 1100 °C. If the portion of completely wetted $Nd_2Fe_{14}B$/$Nd_2Fe_{14}B$ GBs is so low, what is the mechanism for the formation of magnetically isolating Nd-rich layers between $Nd_2Fe_{14}B$ grains which are needed for high performance of the NdFeB-based alloys for permanent magnets?

Can the $Nd_2Fe_{14}B$/$Nd_2Fe_{14}B$ GBs contain the few nanometer thick Nd-rich layers like the prewetting GB layers in metals [17–22,65–70,78,79] or oxides [4–16]? Already in early 1990-ies such few nm thin Nd-rich GB layers were indeed observed in the NdFeB-based alloys [80]. Later the Nd-rich uniformly thick layers between $Nd_2Fe_{14}B$ grains with thickness below 5 nm were observed in various alloys in many experimental works (Fig. 6a) [80–93]. What is the physical reason for the formation of such uniformly thick GB layers of few nm thickness? As we saw above, in the first half of this paper, two possibilities exist for the explanation of this phenomenon. First one is the complete GB wetting by a liquid phase in case of a deficit of a melt. In this case the liquid pockets in the GB triple junctions could still completely wet the TJs and form the continuous network along TJs. The TJ pockets make than the impression that the amount is of a liquid phase is not as low. Nevertheless, the liquid phase distributes in this case in such a way that the pockets in TJs remain macroscopic (i.e. few ìm in diameter) but in GBs the melt is in a deficit and is able to cover the GBs only with a few nm thin films. In this case the liquid in the TG pocket should undergo into a thin GB layer without any shape discontinuity or break of the first shape derivative (like it is shown in the scheme in Fig. 5c). Such continuous shape transition between TJ pocket and GB film has been indeed observed in various experiments [23,82,83,94–97]. In numerous papers one can see in the published micrographs simultaneously TJs with (solidified by cooling) liquid inside and thin film in GBs works (Fig. 7a) [23,80,82-84,90,93–97,113].

Second possible explanation for the existence of the uniformly thin GB layers is the pseudopartial GB wetting (like it is shown in the scheme in Figs. 5a-5c). In this case there should be a shape discontinuity (break of the first shape derivative) in the contact point between liquid TJ pocket and thin GB layer. It is easy to judge about pseudopartial GB wetting if the contact angle is equal or above 60° (like in Figs. 5a and 5b). If the contact angle is small (like it is shown in Fig. 5c), the transition between liquid in TJ and (quasi)liquid in GB is rather smooth, the discontinuity is weak and not easy to distinguish from the case of complete wetting and deficit of a melt (Fig. 5d) like in Fig. 7b taken from Ref. [23]. On the other hand, there are numerous papers where the pseudopartial GB wetting is quite easy

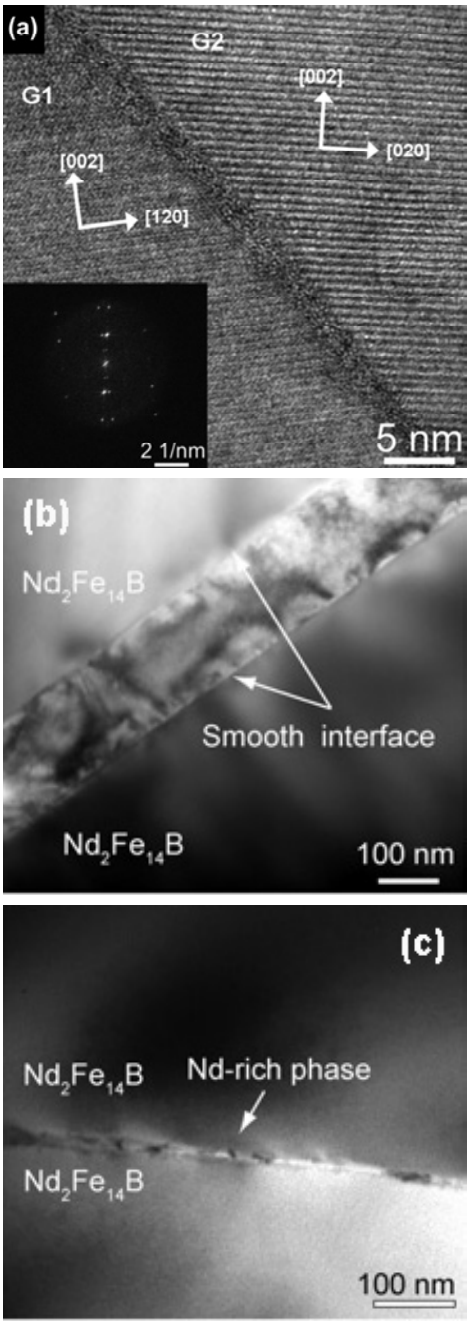

Fig. 6. TEM micrographs showing the uniform Nd-rich layers between $Nd_2Fe_{14}B$ grains (a) with thickness below 5 nm [23]. Reprinted with permission from Elsevier Ltd., © 2013 Acta Materialia Inc. (b) with thickness above 100 nm [97] and (c) with thickness between 15 and 50 nm [97]. Reprinted with permission from Elsevier Ltd., © 2013 Acta Materialia Inc.

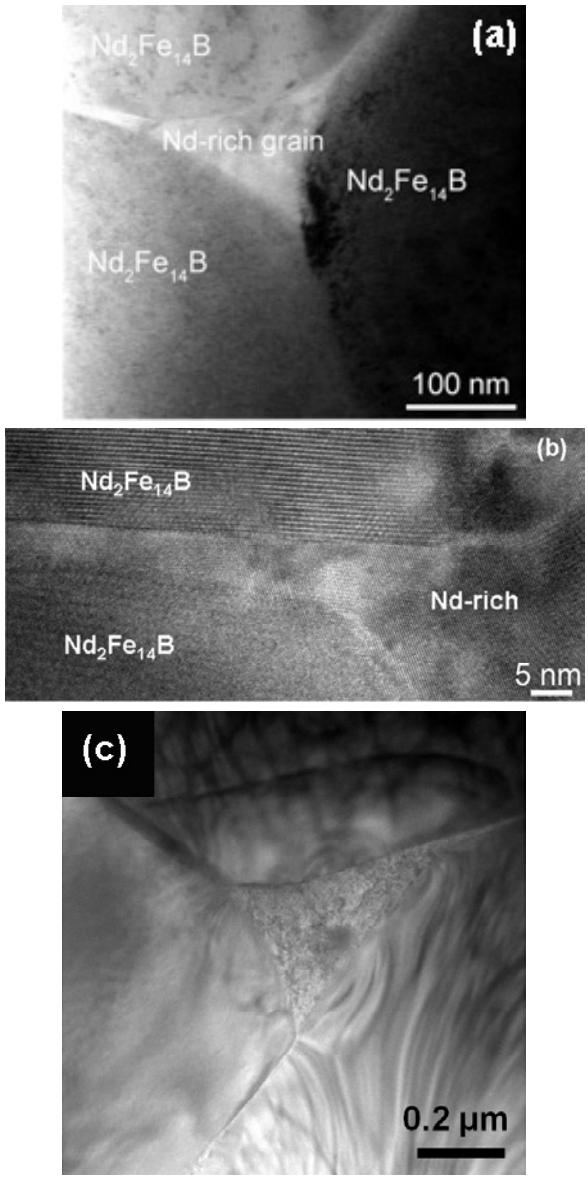

Fig. 7. TEM micrographs simultaneously showing TJs with (solidified by cooling) liquid inside and thin film between $Nd_2Fe_{14}B$ grains. (a) continuous transition between liquid in TJ and (quasi)liquid in GBs [97]. Reprinted with permission from Elsevier Ltd., © 2013 Acta Materialia Inc. (b) the transition between liquid in TJ and (quasi)liquid in GB is rather smooth, the discontinuity is weak and not easy to distinguish from the case of complete wetting and deficit of a melt [23]. Reprinted with permission from Elsevier Ltd., © 2013 Acta Materialia Inc. (c) good visible discontinuity between liquid in TJ and (quasi)liquid in GB [113]. Reprinted with permission from Elsevier Ltd., ©2012 Elsevier B.V.

to observe (Fig. 7c) [80,83,84,90,93,95,96,113]. In this case the discontinuity in the contact point between liquid TJ pocket and thin GB layer is good visible.

In any case, in order to conclude about the nature of thin GB layers one needs the micrographs where both TJ pockets and GB layers are visible. Unfortunately, in the majority of cases the published micrographs of thin Nd-rich GB layers do not contain the places where the GB contacts with a Nd-

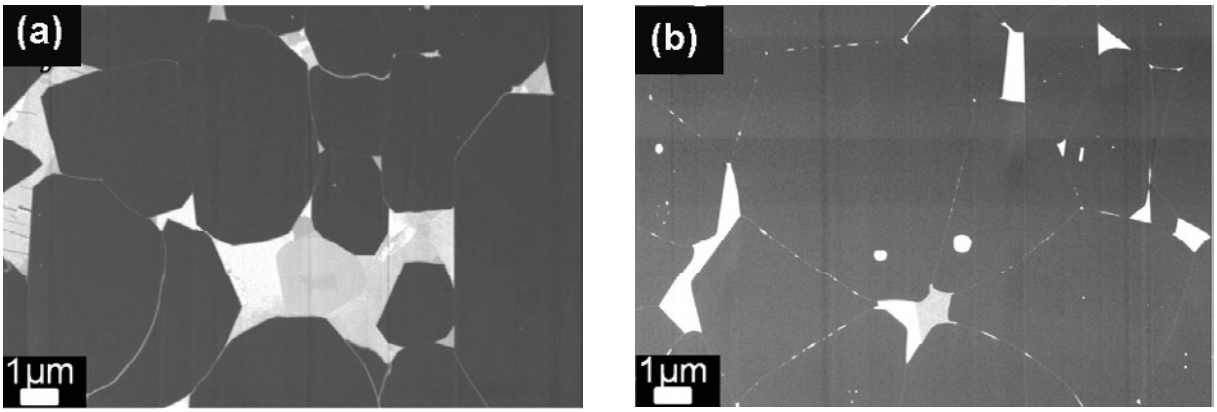

Fig. 8. Low-magnification SEM-micrographs containing numerous GBs and TJs [24]. Reprinted with permission from Elsevier Ltd., © 2013 Acta Materialia Inc. (a) GBs with uniform continuous layers of solidified Nd-rich phase. (b) incompletely wetted GBs (chains of solidified Nd-rich phase particles are visible).

rich pocket in a TJ (Fig. 6a) [23,89,91]. In such cases it is not easy or even not possible to judge, whether we deal with complete GB wetting with deficit of wetting phase or pseudopartial GB wetting. However, in few cases the published micrographs not only show the contact are between TJ and GBs, but also permit to resolve the discontinuity at the contact point between TJ liquid pocket and thin layer of a (quasi)liquid phase in GBs (Fig. 7c) [80,83,84,90,93,95,96,113].

The observation of low-magnification SEM-micrographs containing numerous GBs and TJs of such alloys, on the first glance, does not allow to say that the amount of the liquid phase is small (Figs. 8a and 8b) [24]. On the other hand we only can speak that the amount of the liquid phase is enough to completely wet TJs and to form the continuous network of linear TJs filled by the liquid phase (forming liquid channels). In other words, the amount of this liquid phase is not enough to completely wet the GBs and fill them with thick melted layers [23]. On the other edge of the spectrum of such wetting phenomena is the situation when the amount of the liquid phase is large [34,84,86,98]. In this case not only GBs with $\theta = 0$ (due to the fact that $\sigma_{gb} > 2\sigma_{sl}$) contain thick layer of a melt, but also GBs with small θ. It is because in case if θ and also grain size are small enough the liquid layers from neighbouring TJs meet each other in the middle of a GB (so-called apparently complete GB wetting) [34].

In several papers the micrographs are published where we can see the all possible variants of GB wetting in the liquid phase sintered NdFeB-based polycrystals, namely complete GB wetting with thick integranular layers, complete GB wetting with thin integranular layers (due to the deficit of the liquid phase) and continuous shape transition between liquid in TJ and (quasi)liquid in GB, and pseudopartial GB wetting (with discontinuous shape transition between liquid in TJ and thin GB film), see Fig. 6 [80–98].

The change of temperature of the liquid phase sintering or additional annealing after sintering can lead to the (discussed above) phase transformation between complete and partial (or pseudopartial) GB wetting [99–101]. In many cases an optimal temperature of the additional annealing exists which allows to reach the maximal energy product *HB* [94,99–101]. This fact allows us to suppose that changing the annealing temperature one can change the equilibrium structure of the grain boundary layers and increase the portion of thin integranular films magnetically separating the $Nd_2Fe_{14}B$ grains. It is very well seen [94] that increase of the temperature of additional annealing from 400 °C to 520 °C leads to the transition from partial to complete GB wetting by the Nd-rich phase. It is interesting to underline that in many cases the solid phases in TJs and GBs formed after cooling down to the room temperature have different composition [25,100]. Additional alloying of three-component Nd–Fe–B alloys can improve microstructure, GB wetting behaviour as well as magnetic properties. For example the addition of copper [88] or aluminium and copper [99,101] increases the energy product *HB*. The alloying with Dy can be done using GB diffusion [84,95,102]. In this case the expensive Dy addition is used very economically because Dy dopes and improves only GB layers and almost does not penetrate in the bulk of $Nd_2Fe_{14}B$ grains. The alloying by Tb or Dy and Tb leads to the appearing of pseudopartial GB wetting [90,93,102].

Together with liquid phase sintering, the second most important technology of the production of

NdFeB-based hard magnetic alloys is a compaction of the ribbons obtained by the melt spinning [82,103,104]. Such ribbons possess amorphous or nanocrystalline structure. In this case the $Nd_2Fe_{14}B$ nanograins are formed by the additional annealing at 560–650 °C. These grains are separated one from another with layers of remaining amorphous phase. This amorphous phase can also be considered as a wetting phase between the $Nd_2Fe_{14}B$ nanograins [82] similar to the amorphous wetting phase in nanograined oxides [105,106].

The most mysterious phenomenon, from the viewpoint of GB wetting is the formation of rather thick uniform GB layers of Nd-rich phase between $Nd_2Fe_{14}B$ grains. These layers have thickness between 15 to 50 nm (see Fig. 6c) [83,93,95,96,102,107–109,113]. They cannot be considered as been similar to the 2-5 nm thick GB layers. It is because the layers which are less than 5 nm thick exist due to the interaction between two "$Nd_2Fe_{14}B$/melt" interfaces. Due to this fact one usually designates such layers as quasi-liquid because two abutting grains can interact with each other through the GB layer [5–13]. In turn, this interaction defines the thickness of quasi-liquid GB layer and makes it so uniform. If the GB layer is 15 and 50 nm thick it cannot be considered any more as quasi-liquid and should have the properties of a conventional bulk liquid. From our point of view such layers exist due to the complete GB wetting by a liquid phase. In this case, why they are so uniformly thick if the abutting grains cannot interact through the 15- 50 nm of a melt [83,93,95,96,102,107–109,113]? One possible reason can be the faceting/roughening of GBs or "$Nd_2Fe_{14}B$/melt" interfaces [46,110–112]. In other words, the flat GBs or "$Nd_2Fe_{14}B$/melt" interfaces are parallel to the low-indexed closely-packed planes of the abutting $Nd_2Fe_{14}B$ grains. In this case two flat interfaces would be very stable and form the rather uniformly thick wetting layer of "true" bulk liquid in between. However, this hypothesis needs the additional experimental prove, for example with the aid of selected area electron diffraction in TEM or by EBSD.

4. CONCLUSIONS

The thin intergranular films of a second phase are observed in the last decade in metals, oxides, nitrides, etc. Especially frequently they appear as a result of liquid phase sintering. Thin intergranular films can be either detrimental or beneficial. In any case they drastically change the properties of GBs and of a polycrystal as whole. If they resulted from complete GB wetting by a second (liquid or solid) phase, they can form only in a narrow neighbourhood of a soliudus or solvus lines in the bulk phase diagrams. However, the phenomenon of pseudopartial wetting has been recently predicted and then found (first in the liquid mixtures and then on the solid surfaces). In case of pseudopartial wetting the thin intergranular films can exist in the equilibrium with lenticular GB particles of a second phase. In other words, the thin intergranular films can exist in broad two-phase regions of phase diagrams and could be very useful for various applications. The focused usage of such thin magnetically isolating GB layers can further improve the properties of NdFeB-based hard magnetic alloys.

ACKNOWLEDGEMENTS

This work was supported by the Russian Foundation of Basic Research (contract 13-08-90422), Ukrainian State Fund for Fundamental Research (contract Ф53/112-2013), and Erasmus Mundus programme of EU.

REFERENCES

[1] T. Schrell, J. Fidler and H. Kronmüller // *Phys. Rev.* B**49** (1994) 6100.
[2] D. Goll, M. Seeger and H. Kronmüller // *J. Magn. Magn. Mater.* **185** (1998) 49.
[3] J.G. Dash, H. Fu and J.S. Wettlaufer // *Rep. Prog. Phys.* **58** (1995) 115.
[4] P. Bueno, J. Varela and E. Longo // *J. Eur. Ceram. Soc.* **28** (2008) 505.
[5] J. Luo, Y.M. Chiang and R.M. Cannon // *Langmuir* **21** (2005) 7358.
[6] J. Luo, M. Tang, R. Cannon, C.W. Carter and Y.M. Chiang // *Mater. Sci. Eng. A* **422** (2006) 19.
[7] D.R. Clarke // *J. Am. Ceram. Soc.* **70** (1987) 15.
[8] J. Luo // *Crit. Rev. Solid State Mater. Sci.* **32** (2007) 67.
[9] J. Luo and Y.M. Chiang // *Ann. Rev. Mater. Res.* **38** (2008) 227.
[10] A. Subramaniam, C. Koch, R.M. Cannon and M. Rühle // *Mater. Sci. Eng. A* **422** (2006) 3.
[11] P.R. Cantwell, M. Tang, S.J. Dillon, J. Luo, G.S. Rohrer and M.P. Harmer // *Acta Mater.* **62** (2014) 1.
[12] S.J. Dillon, M. Tang, W. Craig Carter and M.P. Harmer // *Acta. Mater.* **55** (2007) 6208.
[13] M.P. Harmer // *J. Am. Ceram. Soc*. **93** (2010) 301.

[14] B.B. Straumal, S.G. Protasova, A.A. Mazilkin, A.A. Myatiev, P.B. Straumal, G. Schütz, E. Goering and B. Baretzky // *J. Appl. Phys.* **108** (2010) 073923.
[15] B.B. Straumal, A.A. Myatiev, P.B. Straumal, A.A. Mazilkin, S.G. Protasova, E. Goering and B. Baretzky // *JETP Letters* **92** (2010) 396.
[16] B.B. Straumal, A.A. Mazilkin, O.A. Kogtenkova, S.G. Protasova and B. Baretzky // *Phil. Mag. Lett*. **87** (2007) 423.
[17] B. Straumal, R. Valiev, O. Kogtenkova, P. Zieba, T. Czeppe, E. Bielanska and M. Faryna // *Acta Mater*. **56** (2008) 6123.
[18] O.A. Kogtenkova, B.B. Straumal, S.G. Protasova, A.S. Gornakova, P. Zięba and T. Czeppe // *JETP Lett*. **96** (2012) 380.
[19] R.Z. Valiev, M.Yu. Murashkin and B.B. Straumal // *Mater. Sci. Forum* **633** (2009) 321.
[20] R.Z. Valiev, M.Y. Murashkin, A. Kilmametov, B.B. Straumal, N.Q. Chinh and T.G. Langdon // *J. Mater. Sci*. **45** (2010) 4718.
[21] N.Q. Chinh, T. Csanádi, J. Gubicza, R.Z. Valiev, B.B. Straumal and T.G. Langdon // *Mater Sci Forum* **667** (2011) 677.
[22] N.Q. Chinh, T. Csanádi, T. Győri, R.Z. Valiev, B.B. Straumal, M. Kawasaki and T.G. Langdon // *Mater. Sci. Eng. A* **543** (2012) 117.
[23] N.M. Dempsey, T.G. Woodcock, H. Sepehri-Amin, Y. Zhang, H. Kennedy, D. Givord, K. Hono and O. Gutfleisch // *Acta Mater.* **61** (2013) 4920.
[24] H. Sepehri-Amin, T. Ohkubo and K. Hono // *Acta Mater*. **61** (2013) 1982.
[25] E. Bertrand, H. Dobbs, D. Broseta, J. Indekeu, D. Bonn and J. Meunier // *Phys. Rev. Lett.* **85** (2000) 1282.
[26] B.B. Straumal and W. Gust // *Mater. Sci. Forum* **207** (1996) 59.
[27] B.B. Straumal, W. Gust and T. Watanabe // *Mater. Sci. Forum* **294** (1999) 411.
[28] H. Gabrisch, U. Dahmen and E. Johnson // *Microsc. Res. Techn.* **42** (1998) 241.
[29] L. Felberbaum, A. Rossoll and A. Mortensen // *J. Mater. Sci.* **40** (2005) 3121.
[30] D. Empl, L. Felberbaum, V. Laporte, D. Chatain and A. Mortensen // *Acta Mater*. **57** (2009) 2527.
[31] B.B. Straumal, L.M. Klinger and L.S. Shvindlerman // *Acta metall.* **32** (1984) 1355.
[32] B.B. Straumal and L.S. Shvindlerman // *Acta metall*. **33** (1985) 1735.
[33] B.B. Straumal, B.S. Bokstein, A.B. Straumal and A.L. Petelin // *JETP Letters* **88** (2008) 537.
[34] A.B. Straumal, B.S. Bokstein, A.L. Petelin, B.B. Straumal, B. Baretzky, A.O. Rodin and A.N. Nekrasov // *J. Mater. Sci.* **47** (2012) 8336.
[35] W. Beere // *Acta. Metall.* **23** (1975) 131.
[36] J.R. Bulau, H.S. Waff and J.A. Tyburczy // *J. Geophys. Res*. **84** (1979) 6102.
[37] R.M. German // *Metal. Trans. A* **16** (1985) 1247.
[38] Y. Takei // *J. Geophys. Res. B* **8** (1998) 18183.
[39] S.R. Jurewicz and E. B. Watson // *Geochim. Cosmochim. Acta* **49** (1985) 1109.
[40] J. Liu and R.M. German // *Metal. Mater. Trans. A* **32** (2001) 165.
[41] J.F. Nye // *J. Glaciol.* **35** (1989) 17.
[42] J. F. Nye, In: *Physics and Chemistry of Ice*, ed. by N. Maenoa and T. Hondoh (Kokhido University Press, Sapporo, 1992), p. 200.
[43] H. Mader // *J. Glaciol.* **38** (1992) 333.
[44] J.W. Cahn // *J. Chem. Phys.* **66** (1977) 3667.
[45] C. Ebnerand W. F. Saam // *Phys. Rev. Lett.* **38** (1977) 1486.
[46] B.B. Straumal, S.A. Polyakov and E.J. Mittemeijer // *Acta Mater*. **54** (2006) 167.
[47] J. Schölhammer, B. Baretzky, W. Gust, E. Mittemeijer and B. Straumal // *Interf. Sci.* **9** (2001) 43.
[48] B. Straumal, T. Muschik, W. Gust and B. Predel // *Acta Metal. Mater.* **40** (1992) 939.
[49] B. Straumal. G. López, W. Gust and E. Mittemeijer, In: *Nanomaterials by severe plastic deformation. Fundamentals – Processing – Applications*, ed. by M.J. Zehetbauer and R.Z. Valiev (J.Wiley VCH Weinheim, Germany, 2004), p. 642.
[50] L.-S. Chang, C.-H. Yeh and B. B. Straumal // *Rev. Adv. Mater. Sci.* **21** (2009) 1.
[51] A.S. Gornakova, B.B. Straumal, S. Tsurekawa, L.-S. Chang and A.N. Nekrasov // *Rev. Adv. Mater. Sci.* **21** (2009) 18.
[52] B.B. Straumal, A.S. Gornakova, O.A. Kogtenkova, S.G. Protasova, V.G. Sursaeva and B. Baretzky // *Phys. Rev. B* **78** (2008) 054202.

[53] V. Murashov, B. Straumal and P. Protsenko // *Def. Diff. Forum* **249** (2006) 235.
[54] C.-H. Yeh, L.-S. Chang and B.B. Straumal // *Def. Diff. Forum* **258** (2006) 491.
[55] B. Straumal, D. Molodov and W. Gust // *Interface Sci.* **3** (1995) 127.
[56] B. B. Straumal, O. Kogtenkova and P. Zięba // *Acta Mater*. **56** (2008) 925.
[57] G.A. López, E.J. Mittemeijer and B.B. Straumal // *Acta Mater*. **52** (2004) 4537.
[58] B.B. Straumal, A.S. Gornakova, Y.O. Kucheev, B. Baretzky and A.N. Nekrasov // *J. Mater. Eng. Performance* **21** (2012) 721.
[59] B.B. Straumal, Y.O. Kucheev, L.I. Efron, A.L. Petelin, J. Dutta Majumdar and I. Manna // *J. Mater. Eng. Performance* **21** (2012) 667.
[60] B.B. Straumal, B. Baretzky, O.A. Kogtenkova, A.B. Straumal and A.S. Sidorenko // *J. Mater. Sci*. **45** (2010) 2057.
[61] B.B. Straumal, A.S. Gornakova, S.I. Prokofjev, N.S. Afonikova, B. Baretzky, A.N. Nekrasov and K.I. Kolesnikova // *J. Mater. Eng. Perform*. **23** (2014) DOI: 10.1007/s11665-013-0789-3
[62] B.B. Straumal, O.A. Kogtenkova, A.B. Straumal, Yu.O. Kuchyeyev and B. Baretzky // *J. Mater. Sci.* **45** 4271 (2010).
[63] S.G. Protasova, O.A. Kogtenkova, B.B. Straumal, P. Zięba and B. Baretzky // *J. Mater. Sci.* **46** (2011) 4349.
[64] B.B. Straumal and B. Baretzky // *Interf. Sci*. **12** (2004) 147.
[65] E.I. Rabkin, V.N. Semenov, L.S. Shvindlerman and B.B. Straumal // *Acta Metall. Mater.* **39** (1991) 627.
[66] O.I. Noskovich, E.I. Rabkin, V.N. Semenov, B.B. Straumal and L.S. Shvindlerman // *Acta Metall. Mater.* **39** (1991) 3091.
[67] B.B. Straumal, O.I. Noskovich, V.N. Semenov, L.S. Shvindlerman, W. Gust and B. Predel // *Acta Metall. Mater.* **40** (1992) 795.
[68] V.N. Semenov, B.B. Straumal, V.G. Glebovsky and W. Gust // *J. Crystal Growth* **151** (1995) 180.
[69] B. Straumal, E. Rabkin, W. Lojkowski, W. Gust and L.S. Shvindlerman // *Acta Mater.* **45** (1997) 1931.
[70] B. Straumal, E. Rabkin, L. Shvindlerman and W. Gust // *Mater. Sci. Forum.* **126–128** (1993) 391.
[71] F. Brochard-Wyart, J. M. di Meglio, D. Quéré and P. G. de Gennes // *Langmuir* **7** (1991) 335.
[72] P.G. de Gennes // *Rev. Mod. Phys.* **57** (1985) 827.
[73] B.B. Straumal, P. Zieba and W. Gust // *Int. J. Inorg. Mater*. **3** (2001) 1113.
[74] B. Straumal, E. Rabkin, W. Lojkowski, W. Gust and L.S. Shvindlerman // *Acta Mater.* **45** (1997) 1931.
[75] J. Moon, S. Garoff, P. Wynblatt and R. Suter // *Langmuir* **20** (2004) 402.
[76] B.B. Straumal, X. Sauvage, B. Baretzky, A.A. Mazilkin and R.Z. Valiev // *Scripta Mater.* **70** (2014) 59.
[77] B.B. Straumal, Yu.O. Kucheev, I.L. Yatskovskaya, I.V. Mogilnikova, G. Schütz and B. Baretzky // *J. Mater. Sci.* **47** (2012) 8352.
[78] V.K. Gupta, D.H. Yoon, H.M. Meyer and J. Luo // *Acta. Mater.* **55** (2007) 3131.
[79] J. Luo, V.K. Gupta, D.H. Yoon and H.M. Meyer // *Appl. Phys. Lett*. **87** (2005) 231902.
[80] L. Li, D. E. Luzzi and C.D. Graham // *J. Mater. Eng. Perform.* **1** (1992) 205.
[81] N. Watanabe, M. Itakura and M. Nishida // *J. Alloys Comp*. **557** (2013) 1.
[82] Y.-G. Park and D. Shindo // *J. Magn. Magn. Mater.* **238** (2002) 68.
[83] V.V. Volkov and Y. Zhu // *J. Magn. Magn. Mater.* **214** (2000) 204.
[84] H. Sepehri-Amin, T. Ohkubo and K. Hono // *J. Appl. Phys.* **107** (2010) 09A745.
[85] K. Hono and H. Sepehri-Amin // *Scripta Mater*. **67** (2012) 530.
[86] H. Sepehri-Amin, Y. Une, T. Ohkub, K. Hono and M. Sagawa // *Scripta Mater.* **65** (2011) 396.
[87] W.F. Li, H. Sepehri-Amin, T. Ohkubo, N. Hase and K. Hono // *Acta Mater.* **59** (2011) 3061.
[88] H. Sepehri-Amin, T. Ohkub, T. Nishiuchi, S. Hirosawa and K. Hono // *Scripta Mater.* **63** (2010) 1124.
[89] K. Suresh, T. Ohkubo, Y.K. Takahashi, K. Oh-ishi, R. Gopalan, K. Hono, T. Nishiuchi, N. Nozawa and S. Hirosawa // *J. Magn. Magn. Mater.* **321** (2009) 3681.
[90] N. Watanabe, H. Umemoto, M. Ishimaru, M. Itakura, M. Nishida and K. Machida // *J. Microsc.* **236** (2009) 104.
[91] H. Suzuki, Y. Satsu and M. Komuro // *J. Appl. Phys.* **105** (2009) 07A734.
[92] W.F. Li, T. Ohkubo, K. Hono, T. Nishiuchi and S. Hirosawa // *Appl. Phys. Lett.* **93** (2008) 052505.

[93] N. Watanabe, H. Umemoto, M. Itakura, M. Nishida and K. Machida // *IOP Conf. Series, Mater. Sci. Eng.* **1** (2009) 012033.
[94] M. Yan, L.Q. Yu, W. Luo, W. Wang, W.Y. Zhang and Y.H. Wen // *J. Magn. Magn. Mater.* **301** (2006) 1.
[95] N. Oono, M. Sagawa, R. Kasada, H. Matsui and A. Kimura // *Mater. Sci. Forum* **654** (2010) 2919.
[96] Q. Ao, W. Liu and J. Wu // *Mater. Trans.* **46** (2005) 123.
[97] Q. Liu, F. Xu, J. Wang, X. Dong, L. Zhang and J. Yang // *Scripta Mater.* **68** (2013) 687.
[98] Z. Samardžija, P. McGuiness, M. Soderžnik, S. Kobe and M. Sagawa // *Mater. Charact.* **67** (2012) 27.
[99] J. Ni, T. Ma and M. Yan // *J. Magn. Magn. Mater.* **323** (2011) 2549.
[100] T.-H. Kim, S.-R. Lee, D.-H. Kim, S.-N. Kung and T.-S. Jang // *J. Appl. Phys.* **109** (2011) 07A703.
[101] J.J. Ni, T.Y.Ma, Y.R.Wu and M. Yan // *J. Magn. Magn. Mater.* **322** (2010) 3710.
[102] K. Hirota, H. Nakamura, T. Minowa and M. Honshima // *IEEE Trans. Magn*. **42** (2006) 2909.
[103] S. Li, B. Gu, H. Bi, Z. Tian, G. Xie, Y. Zhu and Y. Du // *J. Appl. Phys*. **92** (2002) 7514.
[104] S. Li, Y. Dai, B. X. Gu, Z. Tian and Y. Du // *J. Alloys Comp.* **339** (2002) 202.
[105] B.B. Straumal, S.G. Protasova, A.A. Mazilkin, P.B. Straumal, G. Schütz, Th. Tietze, E. Goering and B. Baretzky // *Beilstein J. Nanotechnol.* **4** (2013) 361.
[106] B.B. Straumal, A.A. Mazilkin, S.G. Protasova, A.A. Myatiev, P.B. Straumal, E. Goering and B. Baretzky // *Phys. Stat. Sol*. B **248** (2011) 581.
[107] J. Ni, T. Ma and M. Yan // *Mater. Lett.* **75** (2012) 1.
[108] H. Sepehri-Amin, T. Ohkubo, T. Shima and K. Hono // *Acta Mater.* **60** (2012) 819.
[109] F. Xu, L. Zhang, X, Dong, Q, Liu and M. Komuro // *Scripta Mater*. **64** (2011) 1137.
[110] B.B. Straumal, S.A. Polyakov, E. Bischoff, W. Gust and E.J. Mittemeijer // *Interface Sci*. **9** (2001) 287.
[111] V.G. Sursaeva, B.B. Straumal, A.S. Gornakova, L.S. Shvindlerman and G. Gottstein // *Acta Mater*. **56** (2008) 2726.
[112] B.B. Straumal, S.A. Polyakov, E. Bischoff, W. Gust and B. Baretzky // *Acta Mater*. **53** (2005) 247.
[113] T.-H. Kim, S.-R. Lee, S. Namkumg and T.-S. Jang // *J. Alloys Comp*. **537** (2012) 261.